



Kent Academic Repository

Varignon, Julien, Bristowe, Nicholas C. and Ghosez, Philippe (2016) *Electric Field Control of Jahn-Teller Distortions in Bulk Perovskites*. *Physical Review Letters*, 116 (5). ISSN 0031-9007.

Downloaded from

<https://kar.kent.ac.uk/60250/> The University of Kent's Academic Repository KAR

The version of record is available from

<https://doi.org/10.1103/PhysRevLett.116.057602>

This document version

Author's Accepted Manuscript

DOI for this version

Licence for this version

UNSPECIFIED

Additional information

Versions of research works

Versions of Record

If this version is the version of record, it is the same as the published version available on the publisher's web site. Cite as the published version.

Author Accepted Manuscripts

If this document is identified as the Author Accepted Manuscript it is the version after peer review but before type setting, copy editing or publisher branding. Cite as Surname, Initial. (Year) 'Title of article'. To be published in *Title of Journal*, Volume and issue numbers [peer-reviewed accepted version]. Available at: DOI or URL (Accessed: date).

Enquiries

If you have questions about this document contact ResearchSupport@kent.ac.uk. Please include the URL of the record in KAR. If you believe that your, or a third party's rights have been compromised through this document please see our [Take Down policy](https://www.kent.ac.uk/guides/kar-the-kent-academic-repository#policies) (available from <https://www.kent.ac.uk/guides/kar-the-kent-academic-repository#policies>).

Electric field control of Jahn-Teller distortions in bulk perovskites

Julien Varignon,^{1,2,*} Nicholas C. Bristowe,^{1,3,*} and Philippe Ghosez¹

¹*Physique Théorique des Matériaux, Université de Liège (B5), B-4000 Liège, Belgium*

²*Unité Mixte de Physique, CNRS, Thales, Université Paris Sud, Université Paris-Saclay, 91767, Palaiseau, France*

³*Department of Materials, Imperial College London, London SW7 2AZ, UK*
(Dated: September 16, 2015)

The Jahn-Teller distortion, by its very nature, is often at the heart of the various electronic properties displayed by perovskites and related materials. Despite the Jahn-Teller mode being non-polar, we devise and demonstrate in the present letter an electric field control of Jahn-Teller distortions in bulk perovskites. The electric field control is enabled through an anharmonic lattice mode coupling between the Jahn-Teller distortion and a polar mode. We confirm this coupling and quantify it through first-principles calculations. The coupling will always exist within the $Pb2_1m$ space group, which is found to be the favoured ground state for various perovskites under sufficient tensile epitaxial strain. Intriguingly, the calculations reveal that this mechanism is not only restricted to Jahn-Teller active systems, promising a general route to tune or induce novel electronic functionality in perovskites as a whole.

Perovskite ABO_3 compounds, and related materials, are fascinating systems exhibiting a diverse collection of properties, including ferroelectricity, magnetism, orbital-ordering, metal-insulator phase transitions, superconductivity and thermoelectricity¹. Despite the wide range of physical behaviour, a common point at the origin of many of them can be identified as being the Jahn-Teller distortion^{2,3}. The Jahn-Teller distortion is itself intimately linked to electronic degrees of freedom, since traditionally it manifests to remove an electronic degeneracy, opening a band gap and favouring a particular orbital ordering, which in turn can affect magnetic ordering. Furthermore it plays an important role, for example, in colossal magnetoresistance phenomena in doped manganites⁴, superconductivity^{5,6} or the strong electronic correlation observed in the thermoelectric $NaCoO_2$ family⁷.

It would be highly desirable, for device functionality for example, to be able to tune the Jahn-Teller distortion and hence its corresponding electronic properties, with the application of an external electric field. However, Jahn-Teller distortions are non-polar and hence not directly tunable with an electric field.

Recently, the concept of “hybrid improper ferroelectricity” has emerged within the community of oxide perovskites^{8–11}. This concept is related to an unusual coupling of lattice modes, giving rise in the free energy expansion to a trilinear term $-\lambda P.R_1.R_2$ linking the polar motion P to two independent non-polar distortions R_1 and R_2 . Such a coupling was identified in various layered perovskites^{8,9,12–15}, metal-organic framework^{16,17} and can even appear in bulk ABO_3 perovskites^{18,19}. Interestingly, in Ruddlesden-Popper compounds^{9,20} and $ABO_3/A'BO_3$ superlattices²¹, this trilinear coupling appeared as a practical way to achieve electric control of non-polar antiferrodistortive (AFD) motions associated to the rotation of the oxygen octahedra (i.e. monitoring P with an electric field will directly and sizeably tune the non-polar modes R_1 and/or R_2).

Following this spirit, achieving an electric field con-

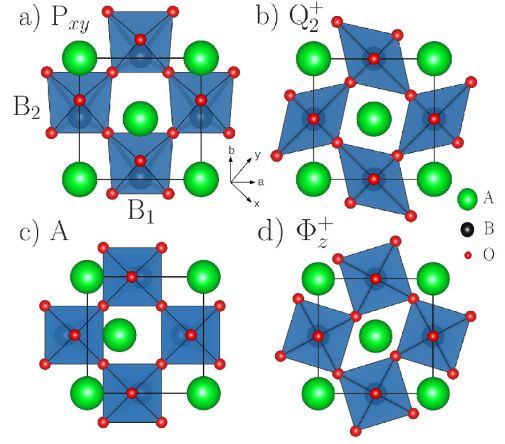


FIG. 1. Schematic view of the main four lattice distortions involved in the $Pb2_1m$ phase of perovskites under tensile epitaxial strain. a) Polar distortion (irreps Γ_5^-) b) Q_2^+ Jahn-Teller distortion (irreps M_3^+) c) Anti-polar A distortion (irreps M_5^+) d) $a^0 a^0 c^+ \phi_z^+$ antiferrodistortive motion (irreps M_2^+).

trol of Jahn-Teller distortions can be realised through the identification of a material exhibiting by symmetry a similar “trilinear” term involving both the polarization and the Jahn-Teller distortion, which to the best of our knowledge has not yet been discovered in bulk ABO_3 perovskites¹¹. In the present letter we identify such conditions, and demonstrate explicitly an electric field control, in bulk perovskites using a combination of symmetry analysis and first-principles calculations.

The two required lattice distortions are pictured in figure 1. a) and b). ABO_3 perovskites often exhibit a non-polar $Pbnm$ ground state, resulting in a combination of three AFD motions ($a^- a^- c^+$ pattern of rotations of the oxygen octahedra in Glazer’s notation²²). In this symmetry, Howard and Carpenter²³ pointed out that a Jahn-Teller distortion pattern automatically appears, which

was later explained in terms of a trilinear coupling with AFD motions^{14,24}. As a consequence, a Jahn-Teller distortion is not necessarily electronically driven, but can instead arise from lattice mode couplings in which case a splitting of the electronic states may develop even in the absence of an electronic instability. The present Jahn-Teller lattice motion corresponds to a Q_2 mode as defined by Goodenough³, corresponding to two B-O bond length contractions and two B-O elongations. This motion orders at the M point of the Brillouin zone and hence consecutive layers along the \vec{c} axis of the $Pbnm$ phase present in-phase distortions. This motion is labelled Q_2^+ throughout the whole manuscript.

Starting from the reference $Pm\bar{3}m$ cubic perovskite phase, the condensation of the polar mode P (irreps Γ_5^-) and the JT mode Q_2^+ (irreps M_3^+) lowers the symmetry to a $Pb2_1m$ phase, a polar subgroup of $Pbnm$. We then perform a free energy expansion²⁵ (around the reference structure) in terms of the lattice distortions allowed by symmetry in this new phase and we identify, among all the possible terms, some intriguing couplings :

$$\mathcal{F} \propto PQ_2^+A + P^2Q_2^+\phi_z^+ + P\phi_z^+A + Q_2^+\phi_z^+A^2 \quad (1)$$

In this phase, the first two terms of equation 1 provide a link between the polarization and the Jahn-Teller distortion. These terms also involve two additional distortions: one anti-polar A motion pictured in figure 1. c) and one $a^0a^0c^+$ AFD motion (labelled ϕ_z^+) pictured in figure 1. d). Among all the terms, the lowest order trilinear term of the form PQ_2^+A provides the desired direct coupling between the polarization and the JT distortion. Thus, acting on the polarization with an external electric field may modify the amplitude of the JT motion, and therefore all related electronic properties.

However, the $Pb2_1m$ symmetry is not the common ground state in bulk perovskites²⁶. Strain engineering, through thin film epitaxy for example, can provide a powerful tool to unlock a polar mode in perovskites^{10,27-32}. This is the case for $BiFeO_3$ which was recently proposed to adopt an unusual $Pb2_1m$ symmetry under large epitaxial tensile strain^{18,33-35}. This particular phase was shown to develop both polar, anti-polar and $a^0a^0c^+$ AFD motions³³, which were later demonstrated to be coupled together through the third term of eq. 1¹⁸. Amazingly, the authors reported the existence of an orbital ordering of the Fe^{3+} $3d$ orbitals, explained from the coexistence of the polar and the anti-polar motion yielding a particular lattice distortion pattern³³. This orbital-ordering is unusual since in this system no Jahn-Teller effect is required to form a Mott insulating state (Fe^{3+} are in a half filled - high spin $t_{2g}^3e_g^2$ configuration). A Jahn-Teller effect or distortion are yet to be reported in the $Pb2_1m$ phase of $BiFeO_3$ to the best of our knowledge. From our symmetry analysis, we clearly demonstrate that as this $Pb2_1m$ develops the three aforementioned distortions (P, A and ϕ_z^+), the free energy of eq. 1 is automatically lowered through the appearance of a fourth lattice distortion: a Jahn-Teller Q_2^+ motion. Therefore, whilst it may not it-

self be unstable, the Jahn-Teller motion is forced into the system via this “improper” mechanism arising from the trilinear coupling⁸. This result clarifies the origin of the unusual orbital-ordering displayed by $BiFeO_3$ and moreover, it provides a pathway to achieve an electric field control of the orbital-ordering in bulk perovskites.

The predicted highly strained $Pb2_1m$ phase in bulk perovskites is not restricted to $BiFeO_3$, and it was predicted to occur also in some titanates ($CaTiO_3$ and $EuTiO_3$)³³, in $BaMnO_3$ ³³ and even in a Jahn-Teller active compound $TbMnO_3$ ³⁶. The highly strained bulk perovskites are then an ideal playground to demonstrate our coupling between the polarization and the Jahn-Teller distortion. In order to check the generality of our concept, we propose in this letter to investigate several types of highly strained perovskites on the basis of first principles calculations: i) non magnetic (NM) $SrTiO_3$ ($t_{2g}^0e_g^0$); ii) magnetic $BaMnO_3$ ³⁷ ($t_{2g}^3e_g^0$) and $BiFeO_3$ ($t_{2g}^3e_g^2$); iii) Jahn-Teller active $YMnO_3$ ($t_{2g}^3e_g^1$).

First-principles calculations were performed with the VASP package^{38,39}. We used the PBEsol⁴⁰+U framework as implemented by Lichtenstein *et al*⁴¹ (see the supplementary material for a discussion on the choice of the U and J parameters). The plane wave cut-off was set to 500 eV and we used a $6 \times 6 \times 4$ k-point mesh for the 20 atom $Pb2_1m$ phase. PAW pseudopotentials⁴² were used in the calculations with the following valence electron configuration: $3s^23p^64s^2$ (Sr), $4s^24p^65s^2$ (Ba), $4s^24p^65s^24d^1$ (Y), $6s^26p^3$ (Bi), $3p^64s^23d^2$ (Ti), $3p^64s^23d^5$ (Mn), $3p^64s^23d^6$ (Fe) and $2s^22p^4$ (O). Spontaneous polarizations were computed using the Berry-phase approach and phonons and Born effective charges were computed using the density functional perturbation theory⁴³. The electric field effect was modelled using a linear response approach by freezing-in some lattice distortion into the system^{44,45}. Symmetry mode analyses were performed using the Amplimodes software from the Bilbao Crystallographic server^{46,47}.

We begin by investigating the possibility of a $Pb2_1m$ ground state under large epitaxial tensile strain (the growth direction is along the [001] axis of the $Pbnm$ structure). Beyond around 5% tensile strain, the four

		$SrTiO_3$	$BaMnO_3$	$BiFeO_3$	$YMnO_3$
strain	(%)	+7.35 ⁴⁸	+6.1 ⁴⁸	+5.8 ⁴⁸	+4.0 ⁴⁸
magnetism		NM	FM	AFMG	AFMG
P (Γ_5^-)	(\AA)	0.615	0.421	0.346	0.753
	($\mu C.cm^{-2}$)	76	45	29	7 ⁴⁹
Q_2^+ (M_3^+)	(\AA)	0.232	0.190	0.644	0.737
A (M_5^+)	(\AA)	0.558	0.217	1.072	0.940
ϕ_z^+ (M_2^+)	(\AA)	0.640	0.059	1.668	1.733
gap	(eV)	3.02	0.28	1.88	1.88

TABLE I. Epitaxial strain (%), magnetic ground state, amplitudes of distortions (\AA) and electronic band gap value (eV) for each material. We emphasize that only the relevant distortions are summarized in the present table.

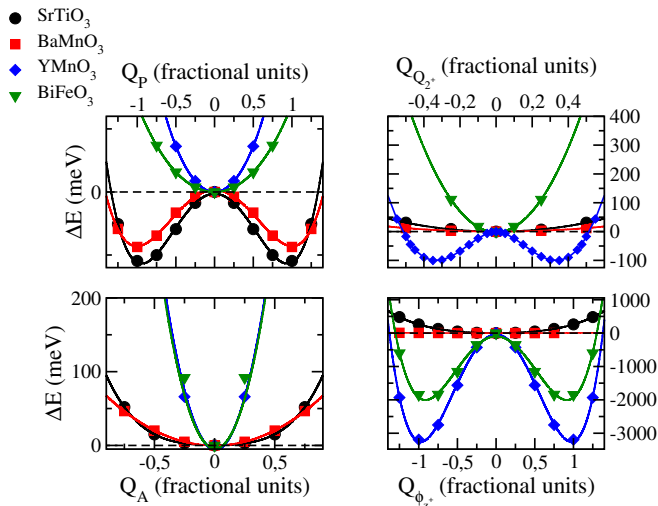


FIG. 2. Potentials with respect to the amplitude of distortions of the four lattice motions producing the required $Pb2_1m$ for SrTiO₃ (black filled circles), BaMnO₃ (red filled squares), YMnO₃ (blue filled diamonds) and BiFeO₃ (green filled triangles) starting from the ideal $P4/mmm$ phase.

compounds indeed develop the desired $Pb2_1m$ ground state. Strained BaMnO₃ (ferromagnetic FM) and YMnO₃ (G-type antiferromagnetic AFMG) exhibit a different magnetic ground state compared to the bulk (AFMG and E-type antiferromagnetic - $\uparrow\uparrow\downarrow\downarrow$ zig-zag chains coupled antiferromagnetically along the \vec{c} axis - respectively) while BiFeO₃ (G-type antiferromagnetic AFMG) remains in its bulk magnetic ground state. We then perform a symmetry mode analysis with respect to a hypothetical $P4/mmm$ phase (corresponding to $Pm\bar{3}m$ for unstrained bulk compounds) in order to extract the amplitude of the relevant lattice distortions⁵⁰ (see table I). As expected, the four materials develop the required distortions, and amazingly, the magnitude of the Q_2^+ Jahn-Teller distortion is relatively large, being for instance of the same order of magnitude as the one developed in the prototypical Jahn-Teller system LaMnO₃ (around 0.265 Å⁵¹). Additionally, the values of the spontaneous polarization are rather large, reaching 76 $\mu C.cm^{-2}$ for SrTiO₃ for instance. Despite being highly strained, all materials remain insulating, adopting reasonable electronic band gap values (see table I).

To shed more light on the origin of this unusual $Pb2_1m$ phase we compute the energy potentials with respect to the four distortions by condensing individually each modes in an hypothetical $P4/mmm$ phase (see figure 2). Surprisingly, the appearance of the $Pb2_1m$ phase is rather different for the four materials. SrTiO₃ and BaMnO₃ only exhibit a polar instability, producing an $Amm2$ symmetry, consistent with previous reports of a polar phase for these two materials under tensile strain^{27,52}. Computing the phonons in this particular $Amm2$ symmetry, only one hybrid unstable phonon mode is identified for these two materials, having a mixed character between

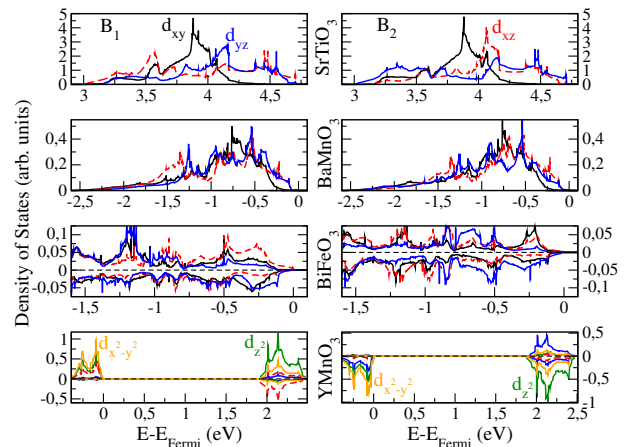


FIG. 3. Projected density of states on the d levels on two neighboring B sites in the (ab) -plane of SrTiO₃, BaMnO₃, BiFeO₃ and YMnO₃. Local axes of the orbitals are displayed on figure 1. The Fermi level is located at 0 eV.

the A, ϕ_z^+ and Q_2^+ distortions. For BiFeO₃ and YMnO₃, the $a^0a^0c^+$ AFD motion is already unstable, which is expected since the $Pb2_1m$ symmetry for these two systems is derived from their bulk $R3c/Pbnm$ phases⁵⁰. Additionally, the JT lattice distortion is also unstable in the $P4/mmm$ phase of YMnO₃ and appears as an electronic instability⁵³, which is expected since YMnO₃ is known to be Jahn-Teller active in the bulk. We emphasize at this stage that the polar mode in BiFeO₃ (and YMnO₃) is not unstable and therefore highly strained BiFeO₃ appears as an improper ferroelectric in contradiction to reference 18⁵⁴. Computing the phonons in the intermediate strained $Pbnm$ phase of both BiFeO₃ and YMnO₃ compounds reveals only one hybrid unstable mode, having a mixed character between P and A distortions. Despite the apparent universal stability of this highly-strained polar phase, the mechanism yielding it is surprisingly different between the compounds and seems linked to the tolerance factor.

Regarding the electronic structure, we checked for the appearance of an orbital ordering as observed in BiFeO₃³³. For the four compounds we report the projected density of states on the d levels of two neighboring B sites in the (ab) -plane (see figure 3). For SrTiO₃, a splitting of the t_{2g} states, and especially between the d_{xz} and d_{yz} orbitals, located at the bottom of the conduction band arises. For BaMnO₃ and BiFeO₃, a similar splitting between the t_{2g} levels is observed near the Fermi level, even if it is less pronounced for BaMnO₃ since it has the smallest Q_2^+ distortion. Finally, YMnO₃ displays an orbital ordering of the e_g levels with predominantly $d_{x^2-y^2}$ occupation. This splitting is known to result from the Jahn-Teller distortion in this $A^{3+}Mn^{3+}O_3$ class of material⁵⁵. Additionally, an orbital ordering of the t_{2g} levels is occurring both in the conduction and the valence bands. To prove that the Jahn-Teller distortion, and not another motion, is solely responsible for the orbital ordering we

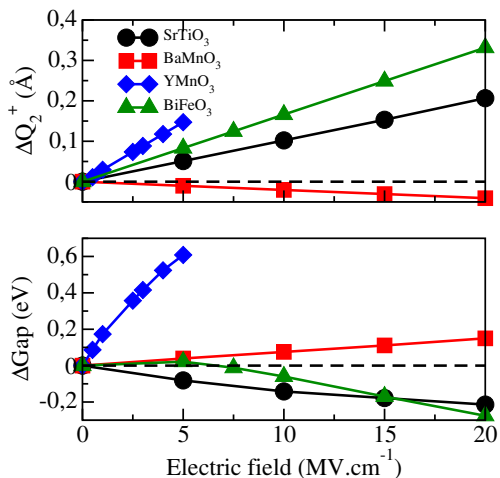


FIG. 4. Electric field effect on the amplitude of the Jahn-Teller distortion (top panel) and the electronic gap value (bottom panel) on the four different compound.

have condensed all the modes individually and studied the density of states (see supplementary figure 1).

Up to here we have demonstrated the existence of a JT distortion and a related orbital ordering in the desired $Pb2_1m$ polar phase. Now, we quantify how the trilinear couplings allow to achieve practical electric field control of the JT distortion. To that end, we compute the magnitude of the JT distortion as a function of the electric field \vec{E} , and exemplify its consequences on the electronic band gap. Results are displayed in figure 4. The Jahn-Teller distortion is effectively tuned by the application of an electric field along the polar axis through the first and second terms of equation 1. As the electric field increases, the amplitude of the JT distortion is either amplified or decreased, being renormalized to around 175% for SrTiO₃ for an electric field around 20 MV.cm⁻¹. The largest effect is however reached for YMnO₃ which displays a renormalization of 130% under moderate electric field (around 5 MV.cm⁻¹). Therefore, this renormalization of the JT distortion has consequences for instance on the electronic band gap value, with an opening/closure

around 0.6 eV for YMnO₃ or 0.25 eV for SrTiO₃. It is then possible, through the coupling between the polarization and the Jahn-Teller distortion to act on the electronic properties.

Here we have exemplified a sizeable electric control of the band gap of direct interest for electro-chromic and photovoltaic applications. Acting directly on the amplitude of the JT distortion might alternatively allow one to control the magnetic state with an electric field, as recently proposed independently in superlattices¹⁴ and metal organic frameworks¹⁶, or to control Metal-Insulator phase transitions.

In conclusion, we have demonstrated in the highly-strained $Pb2_1m$ phase of bulk ABO₃ perovskites the existence of a trilinear coupling involving a polar mode and the Jahn-Teller distortion. This improper anharmonic coupling, established on universal symmetry arguments, enables an electric field control of the Jahn-Teller distortion, even in the case of non-electronically Jahn-Teller active systems. The generic mechanism may open novel functionalities in perovskites as it will have consequences on related electronic properties as proposed in the present Letter. For instance, such couplings may allow the electric control of optical and magnetic properties as well as the tuning of Metal-Insulator phase transitions.

ACKNOWLEDGMENTS

Work supported by the ARC project TheMoTherm and F.R.S-FNRS PDR project HiT4FiT. Ph. Ghosez acknowledges the Francqui Foundation. J. Varignon acknowledges financial support from the ERC Consolidator Grant #615759 MINT. N.C. Bristowe acknowledges the Royal Commission of the Exhibition of 1851 for a fellowship at Imperial College London. Calculations have been performed within the PRACE projects TheoMoMuLaM and TheDeNoMo. They also took advantage of the Céci facilities funded by F.R.S-FNRS (Grant No 2.5020.1) and Tier-1 supercomputer of the Fédération Wallonie-Bruxelles funded by the Walloon Region (Grant No 1117545).

* These two authors contributed equally

¹ P. Zubko, S. Gariglio, M. Gabay, P. Ghosez, and J.-M. Triscone, *Annu. Rev. Condens. Matter Phys.* **2**, 141 (2011).
² H. Köppel, D. R. Yarkony, and H. Barentzen, *The Jahn-Teller Effect* (Springer, 2009).
³ J. Goodenough, *Annual review of materials science* **28**, 1 (1998).
⁴ B. Raveau, M. Hervieu, A. Maignan, and C. Martin, *J. Mater. Chem.* **11**, 29 (2001).
⁵ J. G. Bednorz and K. A. Müller, *Rev. Mod. Phys.* **60**, 585 (1988).
⁶ J. Han, O. Gunnarsson and V. Crespi, *Phys. Rev. Lett.* **90**, 167006 (2003).

⁷ R. Berthelot, D. Carlier and C. Delmas, *Nature Materials* **10**, 74 (2011).
⁸ E. Bousquet, M. Dawber, N. Stucki, C. Lechtensteiger, P. Hermet, S. Gariglio, J. M. Gariglio, and P. Ghosez, *Nature* **452**, 732 (2008).
⁹ N. A. Benedek and C. J. Fennie, *Phys. Rev. Lett.* **106**, 107204 (2011).
¹⁰ J. Varignon, N. C. Bristowe, E. Bousquet, and P. Ghosez, *Comptes Rendus Physique* **16**, 153 (2015).
¹¹ N. A. Benedek, J. M. Rondinelli, H. Djani, Ph. Ghosez and PH. Lightfoot, *Dalton Transactions* (2015).
¹² T. Fukushima, A. Stroppa, S. Picozzi, and J. M. Perez-Mato, *Phys. Chem. Chem. Phys.* **13**, 12186 (2011).

- ¹³ J. M. Rondinelli and C. J. Fennie, *Adv. Materials* **24**, 1961 (2012).
- ¹⁴ J. Varignon, N. C. Bristowe, E. Bousquet, and P. Ghosez, (2014), arXiv preprint arXiv:1409.8422.
- ¹⁵ N. C. Bristowe, J. Varignon, D. Fontaine, E. Bousquet, and P. Ghosez, *Nat. Commun.* **6**, 6677 (2015).
- ¹⁶ A. Stroppa, P. Barone, P. Jain, J. M. Perez-Mato, and S. Picozzi, *Adv. Mater.* **25**, 2284 (2013).
- ¹⁷ Y. Tian, A. Stroppa, Y.-S. Chai, P. Barone, M. Perez-Mato, S. Picozzi, and Y. Sun, *Physica Status Solidi (RRL)* (2014).
- ¹⁸ Y. Yang, J. Íñiguez, A.-J. Mao, and L. Bellaiche, *Phys. Rev. Lett.* **112**, 057202 (2014).
- ¹⁹ Q. Zhou and K. M. Rabe, arXiv preprint arXiv:1306.1839 (2013).
- ²⁰ Ph. Ghosez and J.-M. Triscone, *Nature Materials* **10**, 269 (2011).
- ²¹ Z. Zanoli, J. C. Wojdel, J. Íñiguez, and P. Ghosez, *Phys. Rev. B* **88**, 060102(R) (2013).
- ²² A. Glazer, *Acta Cryst. B* **28**, 3384 (1972).
- ²³ M. A. Carpenter and C. J. Howard, *Acta Cryst. B* **65**, 134 (2009).
- ²⁴ N. Miao, N. C. Bristowe, B. Xu, M. J. Verstraete, and P. Ghosez, *J. Phys.: Cond. Matt.* **26**, 035401 (2014).
- ²⁵ D. M. Hatch and H. T. Stokes, *J. Applied Cryst.* **36**, 951 (2003).
- ²⁶ Being in the $Pb2_1m$ phase is sufficient but *a priori* not mandatory to achieve our goal. From eq 1, only the coupling between the polar and JT distortions is key to achieve an electric field control of the Jahn-Teller distortions. Indeed, one can imagine a metastable phase only developing the antipolar A distortion. Applying an electric field would activate the polar mode and through the first term of eq. 1, the Jahn-Teller distortion may automatically appear. However, in practice this metastable phase does not seem to be favoured, and being in the ground state ferroelectric phase may bring added functionality such as switchable behaviour.
- ²⁷ J. H. Haeni, P. Irvin, W. Chang, R. Uecker, P. Reiche, Y. L. Li, S. Choudhury, W. Tian, M. E. Hawley, B. Craigo, A. K. Tagantsev, X. Q. Pan, S. K. Streiffer, L. Q. Chen, S. W. Kirchoefer, J. Levy, and D. G. Schlom, *Nature* **430**, 758 (2004).
- ²⁸ J. Junquera and P. Ghosez, *J. Comput. Theo. Nanosci.* **5**, 2071 (2008).
- ²⁹ S. Bhattacharjee, E. Bousquet, and P. Ghosez, *Phys. Rev. Lett.* **102**, 117602 (2009).
- ³⁰ T. Günter, E. Bousquet, A. David, P. Boullay, P. Ghosez, W. Prellier, and M. Fiebig, *Phys. Rev. B* **85**, 214120 (2012).
- ³¹ C. J. Fennie and K. M. Rabe, *Phys. Rev. Lett.* **97**, 267602 (2006).
- ³² J. H. Lee, L. Fang, E. Vlahos, X. Ke, Y. W. Jung, L. F. Kourkoutis, J.-W. Kim, P. J. Ryan, T. Heeg, M. Roederath, V. Goian, M. Bernhagen, R. Uecker, P. C. Hammel, K. M. Rabe, S. Kamba, J. Schubert, J. W. Freeland, D. A. M. C. J. Fennie and, P. Schiffer, V. Gopalan, E. Johnston-Halperin, and D. G. Schlom, *Nature* **466**, 954 (2010).
- ³³ Y. Yang, W. Ren, M. Stengel, X. Yan, and L. Bellaiche, *Physical Rev. Lett.* **109**, 057602 (2012).
- ³⁴ Z. Fan, J. Wang, M. B. Sullivan, A. Huan, D. J. Singh, and K. P. Ong, *Scientific Reports* **4** (2014).
- ³⁵ In reference 33, the reported space group for BiFeO_3 under large tensile strain is $Pmc2_1$. This is just an alternative setting of the $Pb2_1m$ space group.
- ³⁶ Y. Hou, J. Yang, X. Gong, and H. Xiang, *Physical Rev. B* **88**, 060406 (2013).
- ³⁷ While the ground state of BaMnO_3 has been shown to adopt a hexagonal polar $P63cm$ structure⁵⁶, BaMnO_3 can also be stabilized with a perovskite form under tensile strain⁵².
- ³⁸ G. Kresse and J. Haffner, *Phys. Rev. B* **47**, 558 (1993).
- ³⁹ G. Kresse and J. Furthmüller, *Computational Materials Science* **6**, 15 (1996).
- ⁴⁰ J. P. Perdew, A. Ruzsinszky, G. I. Csonka, O. A. Vydrov, G. E. Scuseria, L. A. Constantin, X. Zhou, and K. Burke, *Phys. Rev. Lett.* **100**, 136406 (2008).
- ⁴¹ A. I. Liechtenstein, V. I. Anisimov, and J. Zaanen, *Phys. Rev. B* **52**, R5467 (1995).
- ⁴² P. E. Blöchl, *Physical Review B* **50**, 17953 (1994).
- ⁴³ S. Baroni, S. de Gironcoli, A. Dal Corso, and P. Giannozzi, *Rev. Mod. Phys.* **73**, 515 (2001).
- ⁴⁴ J. Íñiguez, *Phys. Rev. Lett.* **101**, 117201 (2008).
- ⁴⁵ J. Varignon, S. Petit, A. Gellé, and M. B. Lepetit, *J. Phys.: Condens. Matt.* **25**, 496004 (2013).
- ⁴⁶ D. Orobengoa, C. Capillas, M. I. Aroyo, and J. M. Perez-Mato, *J. App. Cryst.* **42**, 820 (2009)
- ⁴⁷ J. Perez-Mato, D. Orobengoa, and M. Aroyo, *Acta Cryst. A* **66**, 558 (2010).
- ⁴⁸ The strain percentage is defined as the elongation with respect to the $\sqrt{2}a, \sqrt{2}b$ axes of the pseudo cubic structure corresponding to the fully relaxed ground state. The fully relaxed ground states for all compounds are given in the supplementary materials.
- ⁴⁹ Despite the polar mode amplitude of strained YMnO_3 being similar to the other compounds, the computed polarization is relatively small due to a particular atomic motion pattern of the mode. Indeed, the A and B cations are moving in opposite directions with similar magnitudes, and O motions are nearly canceling each others, resulting in a weak polarization. For the three other compounds, both A and B cations move in opposite direction to O anions, maximizing the polarization.
- ⁵⁰ We only report in table I the relevant distortions for the proposed mechanism. One should notice that due to a small tolerance factor, BiFeO_3 and YMnO_3 still develop large $a^-a^-c^0$ rotations in their ground state, in addition to other antipolar modes. Their $Pb2_1m$ phase may appear to be derived from a $R3c$ or $Pbnm$ structure respectively.
- ⁵¹ J. H. Lee, K. T. Delaney, E. Bousquet, N. A. Spaldin, and K. M. Rabe, *Physical Rev. B* **88**, 174426 (2013).
- ⁵² J. M. Rondinelli, A. S. Eidelson, and N. A. Spaldin, *Phys. Rev. B* **79**, 205119 (2009).
- ⁵³ The JT distortion in YMnO_3 appears through an electronic instability mechanism in the high symmetry phase. Indeed, only removing the symmetry on the electronic wavefunction while keeping the centrosymmetric positions for the cations produces already an energy gain, that is then amplified by the resulting JT lattice distortions.
- ⁵⁴ In reference 18, authors report a relatively weak polar instability in the $P4/mmm$ phase that we do not obtain in our simulations. This contradiction may be related to technical details or the magnitude of the strain applied, but in any case will not affect the final result of the present letter.

⁵⁵ The two average ab-plane Mn-O bond lengths are evaluated to be $\langle d_{MnO} \rangle_{ab,1} = 1.903 \text{ \AA}$ and $\langle d_{MnO} \rangle_{ab,2} = 2.438 \text{ \AA}$ while the average Mn-O bond length along the c axis is around $\langle d_{MnO} \rangle_c = 1.900 \text{ \AA}$. Consequently, the $d_{x^2-y^2}$ orbital should be more stable than the d_{z^2} orbital. Considering

only the sole Q_2^+ distortion, the two in-plane Mn-O bond lengths are 2.294 \AA and 1.772 \AA while the out of plane bond length is 1.769 \AA .

⁵⁶ J. Varignon and P. Ghosez, Phys. Rev. B **87**, 140403(R) (2013).